Overexpression of *miR-19a* inhibits colorectal cancer angiogenesis by suppressing *KRAS* expression

MEIYA CHEN[1], MENGJIE LIN[2] and XIAOZHONG WANG[1]

[1]Department of Gastroenterology, Fujian Medical University Union Hospital, Fuzhou, Fujian 350001;
[2]Department of Pathology, Xiamen University, Zhongshan Hospital, Xiamen, Fujian 361004, P.R. China

Received May 8, 2017; Accepted October 27, 2017

DOI: 10.3892/or.2017.6110

Abstract. The microRNA *miR-19a* is closely related to tumor formation and development and is a key oncogene. Previous studies have demonstrated that *miR-19a* is upregulated in multiple cancer types, including colorectal cancer (CRC). However, most of these experiments were performed *in vitro*, and consequently, the mechanisms underlying the effects of *miR-19a* on CRC are still unclear. Therefore, in the present study, we investigated the role of *miR-19a* in the development of solid CRC tumors. We generated *KRAS* 3'UTR-Mut by deleting the predicted binding site for *miR-19a* in *KRAS*, and observed that the expression of a reporter gene containing the *KRAS* 3'UTR in HCT116 cells was suppressed by *miR-19a*, while that of a reporter gene with mutant *KRAS* 3'UTR was unaffected by *miR-19a*. We observed that high *miR-19a* levels reduced *KRAS* expression. In the tube formation assay, overexpression of *miR-19a* exhibited anti-angiogenesis effects, which were rescued by *KRAS* expression. We established a nude mouse xenograft model to investigate the specific role of *miR-19a* in solid tumors. The results revealed that the sizes of xenograft tumors and density of blood vessels developed from HCT116 cells expressing *miR-19a* were smaller/lower compared with those of the control. KRAS and VEGFA levels were also reduced. In conclusion, our results revealed that *miR-19a* overexpression supressed *KRAS* expression and angiogenesis in CRC, indicating possibilities of using *miR-19a* in future therapeutic applications.

Introduction

Colorectal cancer (CRC) is one of the most common cancers in China, and its incidence rate has increased rapidly in both men and women in recent years (1). Various factors affect the expression of colorectum-specific genes, which contribute to the development and progression of CRC. Mutations and microRNAs (miRNAs) play important roles in the development and progression of CRC. *KRAS* mutations, particularly the activated *KRAS* mutation, induces cell invasion and maintains metastases in CRC, which is considered a landmark event in CRC (2), and patients with *KRAS* mutations have lower survival rates (3). Therefore, targeting *KRAS* is a promising treatment strategy for CRC.

miRNAs play critical roles in CRC tumorigenesis (4). In particular, the following miRNA genes are important: the miR-17-92 cluster consisting of 6 miRNA genes (*miR-17*, *miR-18a*, *miR-19a*, *miR-20a*, *miR-19b-1* and *miR-92a-1*), the *miR-106b-25* and the *miR-106a-363* cluster (5). Previous studies have shown that the *miR-17-92* cluster is upregulated in various human cancers, including CRC (6), and is often thought to play important roles in the development and progression of CRC (7,8).

Among the miRNAs within the *miR-17-92* cluster, *miR-19* functions as a key oncogenic miRNA (9). *miR-19* is comprised of *miR-19a* and *miR-19b*, which share a 96% identity, differing by a single nucleotide at position 11, and are likely to regulate the same mRNA targets. Indeed, *miR-19a* expression has been revealed to be closely related to the development and progression of several types of tumors (10,11). For example, *miR-19a* contributed to the proliferation and invasion of CRC cells (12). Additionally, hsa-*miR-19a* is associated with lymph metastasis and mediates tumor necrosis factor (TNF)-α-induced epithelial-to-mesenchymal transition in CRC (13). *miR-19* mediated inhibition of transglutaminase-2 led to enhanced invasion and metastasis in CRC (14). However, several studies have revealed that *miR-19a* may negatively affect CRC development. For example, Yu *et al* demonstrated that *miR-19a* can suppress tissue factor expression *in vitro* and inhibit colon cancer cell migration and invasion (15). Moreover, most of the experiments reported have been based on *in vitro* cell culture, and few experiments have ascertained the actual role of *miR-19a* in colorectal solid tumors *in vivo*. Thus, the specific role of *miR-19a* in CRC remains unclear.

We identified *KRAS* as one of the target genes of *miR-19a*, using a site-prediction web site, and were interested in investigating the effect of *miR-19a* overexpression in CRC.

In the present study, we aimed to elucidate the precise role and underlying mechanisms of *miR-19a* in CRC, using both

Correspondence to: Professor Xiaozhong Wang, Department of Gastroenterology, Fujian Medical University Union Hospital, 29 Xinquan Road, Fuzhou, Fujian 350001, P.R. China
E-mail: drwangxz@163.com

Key words: *miR-19a*, *KRAS*, angiogenesis, colorectal cancer, VEGFA

Table I. Sequences of primers used in the present study.

Primer	Sequence
miR-19a	
Probe	5'-UCAGUUUUGCAUAGAUUUGCACA-3'
KRAS	
qRT-PCR	5'-ACAGAGAGTGGAGGATGCTTT-3' (forward)
	5'-TTTCACACAGCCAGGAGTCTT-3' (reverse)
hKRAS-3'UTR	5'-CCGTGTAATTCTAGAGCTTATTTTAAAATGACAGTGGAAGT-3' (forward, F1)
	5'-CGCCCCGACTCTAGAGGATAGGGTTCTGTCTATTCATACC-3' (reverse, R1)
hKRAS-3'UTR-M	5'-TTGGATAGCTCAACAAGATACAATCTCACTCTGTGG-3' (forward, F2)
	5'-TGTTGAGCTATCCAAGTCCCTCCCCATTTTGACTA-3' (reverse, R2)
sh-KRAS-1#	5'-AAAAGGATTCCTACAGGAAGCAAGTTTGGATCCAAACTTGCTTCCTGTAGGAATCC-3'
sh-KRAS-2#	5'-AAAAGGACTTAGCAAGAAGTTATGGTTGGATCCAACCATAACTTCTTGCTAAGTCC-3'
sh-control	5'-AAAATACAACAGCCACAACGTCTATTTGGATCCAAATAGACGTTGTGGCTGTTGTA-3'
GAPDH	5'-AGAAGGCTGGGGCTCATTTG-3' (forward)
	5'-AGGGGCCATCCACAGTCTTC-3' (reverse)
U6 probe	5'-CTCGCTTCGGCAGCACA-3'

in vitro assays and an *in vivo* mouse tumor model. We believe that our findings provide important insights into CRC biology and highlight the possibility of using *miR-19a* as a therapeutic agent for CRC in future.

Materials and methods

Study approval. Animal experiments were performed in compliance with the rules of the Animal Use Committee of Fujian Medical University. The present study was approved by the Institutional Ethics Board of Fujian Medical University Union Hospital.

Northern blotting. Northern blotting was performed to detect miRNAs as previously described (16). Briefly, we used RNAiso Plus to extract 10-20 μg total RNA from cells. The RNA was then separated on 10% denaturing polyacrylamide gels and electrotransferred to nylon membranes. DNA oligonucleotides that were antisense to mature miRNAs and end-labeled with ^{32}P were used as probes. U6 snRNA was used as an internal control. A *miR-19a* probe (Pr009177336, 5'-UCAGUUUUGCA UAGAUUUGCACA-3') was used to detect *miR-19a*.

Cell culture and transfection. The human CRC cell line HCT116 (a gift from Professor Pan Jinshui) was cultured in Dulbecco's modified Eagle's medium (DMEM) supplemented with 10% fetal bovine serum (FBS; Gibco Life Technologies, Gaithersburg, MD, USA) and was maintained at 37˚C in a humidified 5% CO_2 atmosphere. The *miR-19a* mimic (5'-UGUGCAAAUCUAUGCAAAACUGA-3'), inhibitor and negative control were purchased from RiBoBio (Guangzhou, China). For transfection, cells ($3x10^5$/well) were cultured in a six-well plate until they reached 40-50% confluency, and the mimics were transfected using Lipofectamine 2000 (Invitrogen, Carlsbad, CA, USA) according to the manufacturer's instructions.

Histology and immunohistochemistry. Hematoxylin and eosin (H&E) staining was performed using standard protocols. Briefly, deparaffinized rehydrated sections were stained with hematoxylin for 5 min, incubated in 0.1% acid alcohol, and then counterstained in 0.5% eosin Y solution. Sections were finally dehydrated and examined by a skilled pathologist. For immunohistochemistry, sections were deparaffinized and quenched with 3% H_2O_2. After the antigen was retrieved in 10 mM sodium citrate buffer and blocked with goat serum (ZLI-9022; ZSGB-BIO, Xicheng, Beijing, China), the sections were incubated with antibodies recognizing CD31 (ab28364; Abcam, Cambridge, UK) or KRAS (12063-1-AP; Proteintech, Chicago, IL, USA) and then with secondary antibodies conjugated with horseradish peroxidase (PV-6101; ZSGB-BIO). Sections were processed according to the manufacturer's instructions and counterstained with hematoxylin.

Western blotting and antibodies. We performed sodium dodecyl sulfate-polyacrylamide gel electrophoresis (SDS-PAGE) to separate total cell lysates, and then transferred the proteins to polyvinylidene difluoride membranes (EMD Millipore, Billerica, MA, USA). Western blotting was performed with the appropriate antibodies, which were visualized by enhanced chemiluminescence in accordance with the manufacturer's instructions (ECL; Millipore).

Quantitative real-time polymerase chain reaction (qRT-PCR). Reverse transcription of total RNA was performed using 4 μg total RNA from HCT116 cells. M-MLV reverse transcriptase (BGI, Shenzhen, China) was used to generate cDNAs. The mRNA level of *KRAS* was assessed by qRT-PCR using SYBR-Green I on a CFX96 real-time RT-PCR detection system (Bio-Rad, Hercules, CA, USA). The sequences of the primers used in the present study are listed in Table I. PCR was performed for 45 cycles using the following conditions: denaturation at 95˚C for 20 sec, annealing at 58˚C for

20 sec, and elongation at 72˚C for 20 sec. All values were normalized to the expression of glyceraldehyde 3-phosphate dehydrogenase (*GAPDH*) mRNA, and the relative expression was calculated according to the ΔΔCT method (17), where $\Delta\Delta CT = \Delta CT_{sample} - \Delta CT_{GAPDH}$.

In vitro tube formation assay. The tube formation efficiency of human umbilical vein endothelial cells (HUVECs) was assessed by an angiogenesis assay on Matrigel (BD Biosciences, Franklin Lakes, NJ, USA). First, we prepared the GFP-labeled HUVECs, as described by Guo *et al* (18), and then 36 h after transfection with *miR-19a*, *KRAS*/*sh-KRAS-2#* or *VEGFA* expression constructs, the HUVECs ($1x10^4$ cells) were added to a 24-well plate coated with 100 μl Matrigel basement membrane matrix (BD Biosciences), which was derived from an Engelbreth-Holm-Swarm tumor. After culturing for 12 h, we recorded tube formation with an IX71 inverted fluorescence microscope (Olympus, Tokyo, Japan) at a low magnification of (x10). Four wells for each treatment were photographed. The images were saved as JPEG files and analyzed using TCS Cellworks AngioSys 1.0 software (Botolph Claydon, Buckingham, UK) to quantify the effects on angiogenesis. Data were analyzed using unpaired Student's t-test of GraphPad Prism 5.0 (GraphPad Software, Inc., La Jolla, CA, USA).

Packaging of lentivirus. For lentivirus packaging, 1.5 μg lentivirus vector was mixed with 1.5 μg packaging plasmids (0.75 μg pMDL, 0.45 μg VSV-G and 0.3 μg REV) in six-well plates. The mixed plasmids were transfected into 293T cells at a density of ~80% confluence using calcium phosphate precipitation. Lentivirus particles were harvested 48 h after transfection. The plasmid pBOB-EGFP was used as a positive control.

Tumorigenesis assay. HCT116 cells were infected using the appropriate amount of lentivirus, and then subjected to amplification. Infected cells were trypsinized and suspended in FBS-free DMEM-F12 medium at a density of $6x10^6$ cells/0.1 ml. The suspended cells were then implanted into the backs of 27 five-week-old BALB/c female nude mice divided into 3 groups, with each group containing nine mice for initiating tumor xenografts. Tumor diameters were measured every 3 days.

DNA constructs. The plv vector carrying a copy of *miR-19a* or *VEGFA* was a kind gift from Dr Lixin Hong (School of Life Science, Xiamen University, Fujian, China). The pGL3 control vector carrying a 1,923-bp fragment of the 3'UTR of human *VEGFA* mRNA was directly purchased from RiBoBio. The *KRAS* 3'UTR harboring predicted target sites for *miR-19a* (Fig. 1A) was PCR-amplified using primers containing *Xba*I sites and cloned into the *Xba*I-digested pGL3 control vector. The recombinant plasmids were constructed using ligation-independent combination (LIC). F1 and R1 primers were used to generate the *KRAS* wild-type 3'UTR. To construct 3'UTRs with deletion mutations, two sets of PCR were performed using the primer pairs F1/R2 and F2/R1 to generate two fragments. Then, the two fragments were cloned into the *Xba*I-digested pGL3 control vector using LIC.

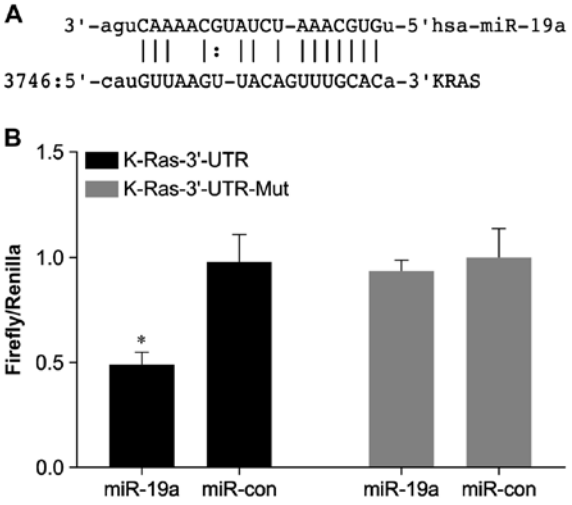

Figure 1. *KRAS* is a target of *miR-19a* in HCT116 cells. (A) The target site for *miR-19a* in human *KRAS*. (B) HCT116 cells were transfected with a vector encoding the firefly luciferase reporter gene containing the *KRAS* 3'UTR or a mutant (Mut) 3'UTR, the *miR-19a* binding site of which was deleted, and with a *Renilla* luciferase control reporter vector and a *miR-19a* expression vector. Firefly luciferase activity was normalized to the *Renilla* luciferase activity (Firefly/*Renilla*). The results are presented as the mean ± SD (n=3); *P<0.05 vs. miR-con.

The DNA oligos encoding shRNA sequences were designed and cloned into the expression vector pLV-H1-EF1α-puro using single oligonucleotide RNAi technology developed by Biosettia (San Diego, CA, USA). All lentiviral-shRNA vectors were constructed following the manufacturer's protocol. The primers used in the present study are listed in Table I.

Dual-luciferase reporter assay. HCT116 cells were plated in six-well culture plates 24 h before transfection. The cells were then transfected with the recombinant pGL3 vector (1.6 μg), plv-*miR-19a* (0.2 μg) and the pRLTK vector (0.2 μg) for normalization of transfection efficiency. Cell lysates were collected and assayed 48 h after transfection. Firefly and *Renilla* luciferase activities were determined using a Dual-Luciferase Reporter Assay System (Promega, Madison, WI, USA). Firefly luciferase activities were calculated as the mean ± standard deviation (SD) after normalization to *Renilla* luciferase activity. Three independent experiments were performed.

Statistical analysis. Mann-Whitney tests were performed to compare the differences between two groups when variances were unequal. Analysis of variance with post hoc tests were performed when comparing >2 groups. For qualitative data, non-parametric tests such as Kruskal-Wallis tests were performed.

Results

miR-19a suppresses KRAS expression in HCT116 cells. We identified the conserved *miR-19a*-binding site in the 3'UTR region of human *KRAS* using the microRNA.org website (Fig. 1A). The *KRAS* 3'UTR-Mut was generated by deleting the predicted binding site. We observed that a reporter gene containing the *KRAS* 3'UTR was suppressed by *miR-19a*,

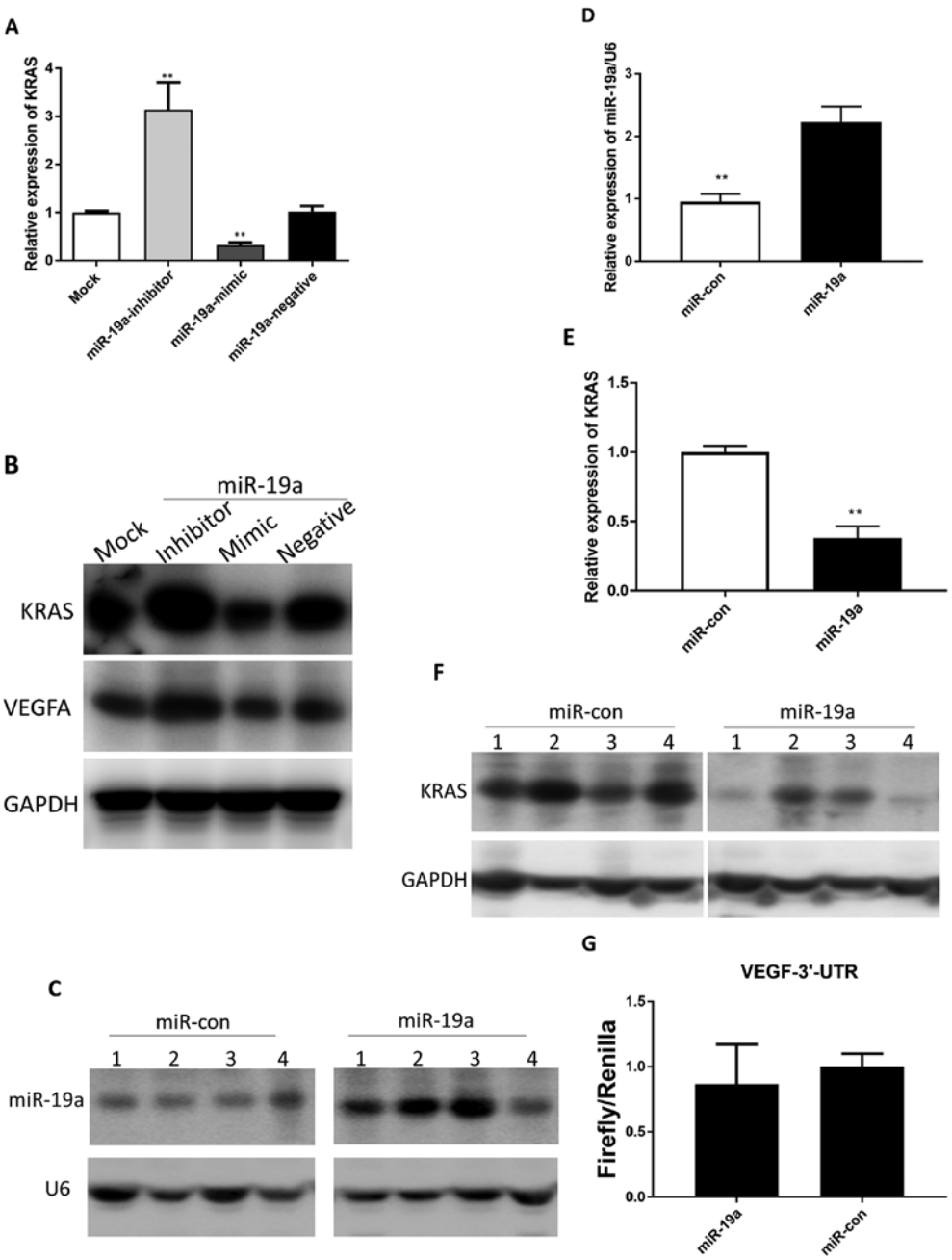

Figure 2. *miR-19a* negatively regulates *KRAS* mRNA and protein levels in human colorectal cancer cells. (A) HCT116 cells were transfected with *miR-19a* mimic/inhibitor, and the levels of *KRAS* mRNA were detected by RT-PCR. The results are presented as the mean ± SD (n=3); **P<0.01 vs. *miR-19a* negative. (B) Western blotting revealed the changes in KRAS and VEGFA protein levels in HCT116 cells. Data from 3 experiments and loading controls are listed below. (C) RNA blot of the expression of *miR-19a* in HCT116 cells with plv-*miR-19a* or plv-miR-con vector. Data from 3 experiments, U6 and loading controls are listed below. (D) The RNA blot was quantified using a Molecular Dynamics Storm 860 phosphorimager; the miRNA expression was normalized to that of U6. (E) In HCT116 cells with the plv-*miR-19a* vector, the expression level of *KRAS* mRNA was downregulated by *miR-19a* overexpression. (F) In HCT116 cells with the plv-*miR-19a* vector, the KRAS protein level was reduced by *miR-19a* overexpression. (G) HCT116 cells were transfected with a vector encoding the firefly luciferase reporter gene containing the *VEGFA* 3'UTR and with a *Renilla* luciferase control reporter vector and a *miR-19a* expression vector. Firefly luciferase activity was normalized to the *Renilla* luciferase activity (Firefly/*Renilla*). The results are presented as the mean ± SD (n=3).

while removal of the predicted *miR-19a*-binding site resulted in insensitivity of the reporter gene to *miR-19a* in HCT116 cells (Fig. 1B).

To ascertain the effect of *miR-19a* on *KRAS* expression in HCT116 cells, the mature *miR-19a* mimic/inhibitor was transfected in HCT116 cells. The results revealed that the endogenous *KRAS* mRNA and protein levels were significantly downregulated in the *miR-19a* mimic cells and upregulated in the *miR-19a* inhibitor cells compared with those in the untransfected cells (Fig. 2A and B). Accordingly, the VEGFA protein level was also downregulated in the *miR-19a* mimic cells and upregulated in the *miR-19a* inhibitor cells (Fig. 2B).

Next, in order to construct stable *miR-19a*-overexpressing HCT116 cell lines for subsequent studies, we transfected HCT116 cells with a lentivirus expressing *miR-19a*. Then, via northern blotting, we confirmed *miR-19a* overexpression in HCT116 cells (Fig. 2C and D). Next, we compared the levels of *KRAS* expressed in HCT116 cells with and without

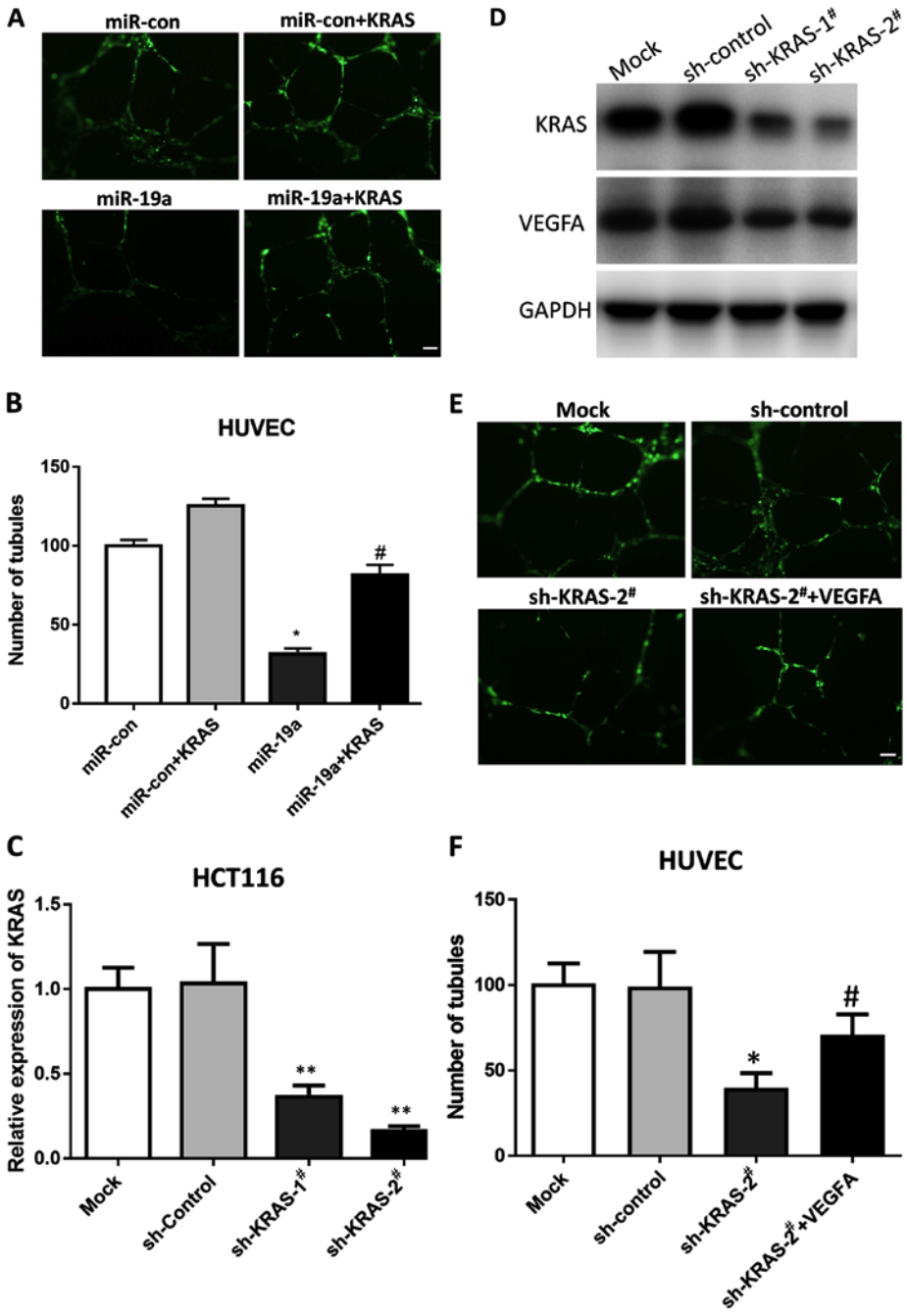

Figure 3. *miR-19a* targets *KRAS* inhibiting tube formation *in vitro*. (A) GFP-labeled HUVECs were transfected with the expression vector miR-con or *miR-19a* as indicated, with or without co-transfection with a *KRAS* expression vector. Representative images are shown; scale bar, 100 μm. (B) Quantitative tube formation data from A. Four wells were photographed for each treatment, and the cells were analyzed to quantify angiogenesis; *P<0.01 vs. miR-con, $^{\#}$P<0.01 vs. *miR-19a*. (C) RT-PCR analysis confirmed that *KRAS* was knocked down by shRNA in HCT116 cells. The results are presented as the mean ± SD (n=3); **P<0.01 vs. sh-control. (D) Western blotting revealed that *KRAS* was knocked down by shRNA in HCT116 cells. Data from 3 experiments and loading controls are listed below. (E) GFP-labeled HUVECs were transfected with the expression vector sh-*KRAS*-2$^{\#}$ or sh-control as indicated, with or without co-transfection with the *VEGFA* expression vector. Representative images are shown; scale bar, 100 μm. (F) Quantitative tube formation data from E. Four wells were photographed for each treatment, and the cells were analyzed to quantify angiogenesis; *P<0.01 vs. sh-control, $^{\#}$P<0.01 vs. sh-*KRAS*-2$^{\#}$.

lentiviral transfection for overexpression of *miR-19a*. The resulting *in vitro* data revealed that overexpression of *miR-19a* decreased *KRAS* mRNA and protein levels in HCT116 cells compared with that in the control (miR-Con; Fig. 2E and F).

TargetScan analysis revealed that *VEGFA* was not a *miR-19a* target. Since the sites that match the miRNA seed sequence are located in 3'UTRs in most mammalian mRNAs, we performed the dual-luciferase reporter assay to detect whether *miR-19a* bound to the 3'UTR of *VEGFA*. The results revealed that the reporter gene containing the *VEGFA* 3'UTR was not suppressed by *miR-19a*, which confirmed that *VEGFA* was not directly regulated by *miR-19a* in HCT116 cells (Fig. 2G).

miR-19a suppresses tube formation by targeting KRAS in vitro. Since high levels of *miR-19a* downregulates *KRAS*, we hypothesized that *miR-19a* may affect angiogenesis. Hence, we performed tube formation assays using HUVECs, which

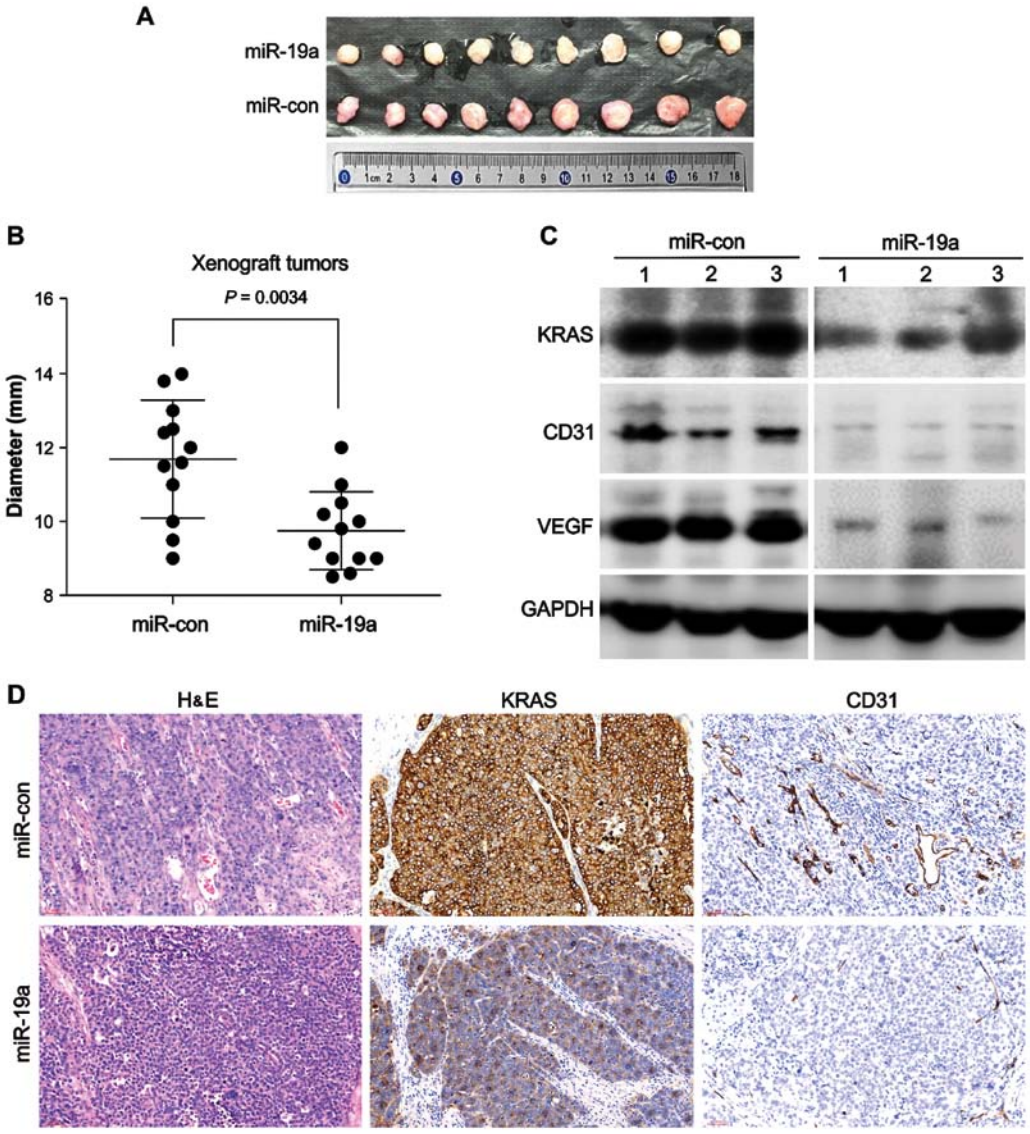

Figure 4. *miR-19a* suppresses angiogenesis by targeting *KRAS in vivo*. (A) Nude mice were injected subcutaneously with $6x10^6$ HCT116 cells. After 24 days, the tumors were removed from the mice. A representative image of the xenograft tumors is shown. (B) The growth of xenograft tumors in nude mice was suppressed by *miR-19a* overexpression (P=0.0034; Student's t-test). (C) Western blotting indicated that KRAS, CD31 and VEGFA protein levels were reduced in tumors overexpressing *miR-19a*. (D) H&E staining revealed that tumors overexpressing *miR-19a* had fewer vessels. A similar result was achieved using immunohistochemical staining of CD31, and KRAS expression was reduced in tumors with *miR-19a* overexpression.

differentiate and form capillary-like structures on Matrigel, to mimic the process via which endothelial cells form capillaries *in vivo* (19). The results revealed that overexpression of *miR-19a* significantly (P<0.01) inhibited angiogenesis in the Matrigel assay, and that rescuing *KRAS* expression could restore angiogenesis inhibited by *miR-19a* (Fig. 3A and B). This confirmed our hypothesis that *miR-19a* suppressed angiogenesis by targeting *KRAS*.

KRAS is a key regulator in VEGF-related angiogenesis. A previous study revealed that the vascular endothelial growth factor receptor (VEGFR) signaling pathway plays a major role in angiogenesis (20) and that KRAS plays a key role in VEGF signaling (21). To ascertain these results, we knocked down *KRAS* using shRNA and determined the expression level of VEGFA in HCT116 cells. The results revealed that two *KRAS* shRNAs reduced *KRAS* mRNA and protein levels significantly, and consequently, VEGFA was also downregulated (Fig. 3C and D). Furthermore, we knocked down *KRAS* using shRNA in HUVECs and performed the tube formation assay. As shown in Fig. 3E, *KRAS* knockdown disrupted tube formation, whereas re-expression of *VEGFA* rescued the defect. Thus, the results demonstrated that *KRAS* was a key regulator of *VEGFA* expression and angiogenesis.

miR-19a suppresses CRC tumor growth in nude mice. The above data indicated that *miR-19a* overexpression could target *KRAS* in HCT116 cells and inhibit tube formation. Therefore, we next examined whether overexpression of *miR-19a* could suppress CRC progression by blocking angiogenesis via targeting of *KRAS* using a xenograft model.

We transplanted the transfected cells into the flanks of nude mice. The results revealed that the sizes of xenograft tumors that developed from HCT116 cells expressing *miR-19a* were much smaller than those from HCT116 cells transfected with the control lentivirus (Fig. 4A and B). In addition, tumors that

developed from *miR-19a*-expressing lentivirus-transfected cells tended to be paler in color than xenograft tumors developed from control lentivirus-transfected cells, indicating decreased blood flow in *miR-19a*-expressing tumors (Fig. 4A).

We performed H&E staining to examine the blood vessels in these tumors. We observed that tumors that developed from *miR-19a*-expressing cells had fewer blood vessels than the control tumors. Immunohistochemical staining for CD31, a marker of vascular endotheliocytes, also revealed that the blood vessels in tumors that developed from *miR-19a*-expressing cells were smaller than those in the control group (Fig. 4D). Moreover, immunohistochemical staining for KRAS and western blotting analysis confirmed that the tumors that developed from *miR-19a*-expressing cells exhibited reduced KRAS expression compared with those in the control group (Fig. 4C and D). Moreover, western blotting analysis revealed that the expression level of VEGFA in tumors that developed from *miR-19a*-expressing cells was also reduced (Fig. 4C). These results indicated that overexpression of *miR-19a* inhibited *KRAS* expression in CRC, which may reduce the production of VEGFA and suppress tumor angiogenesis, thereby delaying tumor growth.

Discussion

In the present study, we evaluated the role of *miR-19a* in colorectal cancer (CRC) development and progression, and observed that overexpression of *miR-19a* resulted in the inhibition of CRC angiogenesis owing to reduced expression of *KRAS*, a known oncogene that has been demonstrated to be a target of *miR-19a* in chronic myeloid leukemia (22).

A study in 2010 revealed that overexpression of *miR-17*, *miR-18a*, *miR-19a* and *miR-20a* considerably inhibited three-dimensional spheroid sprouting *in vitro* (23). Additionally, Landskroner-Eiger *et al* suggested that *miR-19* of the *miR-17-92* family may negatively affect the formation of arterial blood vessels (13). Hence, we hypothesized that *miR-19a* inhibited angiogenesis. In the present study, we revealed that overexpression of *miR-19a* reduced *KRAS* expression in the HCT116 cell line and inhibited angiogenesis, as determined by an *in vitro* tube formation assay. This inhibition, which could be rescued by *KRAS*, consequently slowed down xenograft tumor growth. Hence, we believe that *miR-19a* may be closely related to CRC angiogenesis, and that the anti-angiogenesis effect results from the targeting of *KRAS* by a microRNA. To the best of our knowledge, this is the first study to investigate the primary function of *miR-19a* in solid CRC tumors and to provide a theoretical foundation for the application of miRNA treatment to CRC.

Vascular supply is key for tumor development (24) in various types of cancers, including CRC. Vascular endothelial growth factor (VEGF) and the VEGF receptor pathway play key roles in tumor angiogenesis (25). VEGF/VEGF receptor activation can initiate a signaling cascade that promotes endothelial cell proliferation, migration and differentiation (26). VEGF can also be secreted by CRC cells (27), and it induces angiogenesis. *KRAS* and VEGF have a close relationship. KRAS activation significantly enhances the production of angiogenic factors, including CXC chemokines and VEGF (28), and *KRAS* mutations significantly increase VEGF production (29). Therefore, *KRAS* and VEGF may be involved in creating tumor vascular networks.

Moreover, previous studies have shown a pivotal role of *KRAS* in human cancer development (30) and demonstrated that *KRAS* mutations were indicative of poor prognosis in CRC (31). Therefore, targeting *KRAS* is a promising therapeutic strategy for CRC treatment, particularly for patients with mutations in *KRAS*, which are common in CRC (32). Use of miRNAs for degrading *KRAS* holds promise. For most mammalian mRNAs, the sites that match the miRNA seed sequence (nucleotides 2-7), particularly those in 3'UTRs, are preferentially conserved (33). Therefore, miRNA therapy is unlikely to be affected by gene variations.

Our findings in the present study provided important insights into the role of *miR-19a* in cancer and laid the foundation for future research in this area. High *miR-19a* levels reduced *KRAS* expression and affected angiogenesis in CRC. Thus, *miR-19a* may have applications as a therapeutic agent. However, the present study has one limitation. The *in vitro* analyses were only performed in HCT116 cells, and additional studies using other CRC cell lines are required. With greater and improved understanding of the role of *miR-19a* in CRC, the usefulness of this microRNA in the diagnosis and treatment of CRC may be maximized.

Acknowledgements

The plv vector carrying copies of *miR-19a* and *VEGFA* was a kind gift from Dr Lixin Hong (School of Life Science, Xiamen University, Fujian, China). We are grateful to Professor Pan Jinshui (Xiamen University Zhongshan Hospital, Fujian, China) for kindly providing the HCT116 cell line. The present study was supported by the Key Clinical Specialty Discipline Construction program of Fujian, P.R. China (grant no. 2012-149).

References

1. Chen W, Zheng R, Baade PD, Zhang S, Zeng H, Bray F, Jemal A, Yu XQ and He J: Cancer statistics in China, 2015. CA Cancer J Clin 66: 115-132, 2016.
2. Boutin AT, Liao WT, Wang M, Hwang SS, Karpinets TV, Cheung H, Chu GC, Jiang S, Hu J, Chang K, *et al*: Oncogenic *Kras* drives invasion and maintains metastases in colorectal cancer. Genes Dev 31: 370-382, 2017.
3. Taieb J, Le Malicot K, Shi Q, Penault Lorca F, Bouché O, Tabernero J, Mini E, Goldberg RM, Folprecht G, Luc Van Laethem J, *et al*: Prognostic value of BRAF and *KRAS* mutations in MSI and MSS stage III colon cancer. J Natl Cancer Inst 109: pii: djw272, 2016.
4. Yi R, Li Y, Wang FL, Miao G, Qi RM and Zhao YY: MicroRNAs as diagnostic and prognostic biomarkers in colorectal cancer. World J Gastrointest Oncol 8: 330-340, 2016.
5. He L, Thomson JM, Hemann MT, Hernando-Monge E, Mu D, Goodson S, Powers S, Cordon-Cardo C, Lowe SW, Hannon GJ, *et al*: A microRNA polycistron as a potential human oncogene. Nature 435: 828-833, 2005.
6. Lanza G, Ferracin M, Gafà R, Veronese A, Spizzo R, Pichiorri F, Liu CG, Calin GA, Croce CM and Negrini M: mRNA/microRNA gene expression profile in microsatellite unstable colorectal cancer. Mol Cancer 6: 54, 2007.
7. Diosdado B, van de Wiel MA, Terhaar Sive Droste JS, Mongera S, Postma C, Meijerink WJ, Carvalho B and Meijer GA: MiR-17-92 cluster is associated with 13q gain and c-myc expression during colorectal adenoma to adenocarcinoma progression. Br J Cancer 101: 707-714, 2009.
8. Ma H, Pan JS, Jin LX, Wu J, Ren YD, Chen P, Xiao C and Han J: MicroRNA-17~92 inhibits colorectal cancer progression by targeting angiogenesis. Cancer Lett 376: 293-302, 2016.

9. Olive V, Bennett MJ, Walker JC, Ma C, Jiang I, Cordon-Cardo C, Li QJ, Lowe SW, Hannon GJ and He L: *miR-19* is a key oncogenic component of *mir-17-92*. Genes Dev 23: 2839-2849, 2009.
10. Yamamoto K, Ito S, Hanafusa H, Shimizu K and Ouchida M: Uncovering direct targets of *miR-19a* involved in lung cancer progression. PLoS One 10: e0137887, 2015.
11. Lu WD, Zuo Y, Xu Z and Zhang M: MiR-19a promotes epithelial-mesenchymal transition through PI3K/AKT pathway in gastric cancer. World J Gastroenterol 21: 4564-4573, 2015.
12. Zhang J, Xiao Z, Lai D, Sun J, He C, Chu Z, Ye H, Chen S and Wang J: miR-21, miR-17 and miR-19a induced by phosphatase of regenerating liver-3 promote the proliferation and metastasis of colon cancer. Br J Cancer 107: 352-359, 2012.
13. Landskroner-Eiger S, Qiu C, Perrotta P, Siragusa M, Lee MY, Ulrich V, Luciano AK, Zhuang ZW, Corti F, Simons M, *et al*: Endothelial miR-17~92 cluster negatively regulates arteriogenesis via miRNA-19 repression of WNT signaling. Proc Natl Acad Sci USA 112: 12812-12817, 2015.
14. Cellura D, Pickard K, Quaratino S, Parker H, Strefford JC, Thomas GJ, Mitter R, Mirnezami AH and Peake NJ: miR-19-mediated inhibition of transglutaminase-2 leads to enhanced invasion and metastasis in colorectal cancer. Mol Cancer Res 13: 1095-1105, 2015.
15. Yu G, Li H, Wang X, Wu T, Zhu J, Huang S, Wan Y and Tang J: MicroRNA-19a targets tissue factor to inhibit colon cancer cells migration and invasion. Mol Cell Biochem 380: 239-247, 2013.
16. Xiao C, Calado DP, Galler G, Thai TH, Patterson HC, Wang J, Rajewsky N, Bender TP and Rajewsky K: MiR-150 controls B cell differentiation by targeting the transcription factor c-Myb. Cell 165: 1027, 2016.
17. Livak KJ and Schmittgen TD: Analysis of relative gene expression data using real-time quantitative PCR and the $2^{-\Delta\Delta CT}$ method. Methods 25: 402-408, 2001.
18. Guo H, Jia Y, Shang M, Zhang Y, Xie F, Wang H, Yuan M, Yuan L and Ye J: Comparison of two in vitro angiogenesis assays for evaluating the effects of netrin-1 on tube formation. Acta Biochim Biophys Sin 46: 810-816, 2014.
19. Ponce ML: Tube formation: An in vitro matrigel angiogenesis assay. Methods Mol Biol 467: 183-188, 2009.
20. Simons M and Eichmann A: Molecular controls of arterial morphogenesis. Circ Res 116: 1712-1724, 2015.
21. Yeh YW, Cheng CC, Yang ST, Tseng CF, Chang TY, Tsai SY, Fu E, Chiang CP, Liao LC, Tsai PW, *et al*: Targeting the VEGF-C/VEGFR3 axis suppresses Slug-mediated cancer metastasis and stemness via inhibition of KRAS/YAP1 signaling. Oncotarget 8: 5603-5618, 2017.
22. Chakraborty C, Sharma AR, Patra BC, Bhattacharya M, Sharma G and Lee SS: MicroRNAs mediated regulation of MAPK signaling pathways in chronic myeloid leukemia. Oncotarget 7: 42683-42697, 2016.
23. Doebele C, Bonauer A, Fischer A, Scholz A, Reiss Y, Urbich C, Hofmann WK, Zeiher AM and Dimmeler S: Members of the microRNA-17-92 cluster exhibit a cell-intrinsic antiangiogenic function in endothelial cells. Blood 115: 4944-4950, 2010.
24. Mihalache A and Rogoveanu I: Angiogenesis factors involved in the pathogenesis of colorectal cancer. Curr Health Sci J 40: 5-11, 2014.
25. Shinkaruk S, Bayle M, Laïn G and Déléris G: Vascular endothelial cell growth factor (VEGF), an emerging target for cancer chemotherapy. Curr Med Chem Anticancer Agents 3: 95-117, 2003.
26. Ikeda N, Nakajima Y, Sho M, Adachi M, Huang CL, Iki K, Kanehiro H, Hisanaga M, Nakano H and Miyake M: The association of K-ras gene mutation and vascular endothelial growth factor gene expression in pancreatic carcinoma. Cancer 92: 488-499, 2001.
27. Qiu Y, Yu H, Shi X, Xu K, Tang Q, Liang B, Hu S, Bao Y, Xu J, Cai J, *et al*: microRNA-497 inhibits invasion and metastasis of colorectal cancer cells by targeting vascular endothelial growth factor-A. Cell Prolif 49: 69-78, 2016.
28. Matsuo Y, Campbell PM, Brekken RA, Sung B, Ouellette MM, Fleming JB, Aggarwal BB, Der CJ and Guha S: *K-Ras* promotes angiogenesis mediated by immortalized human pancreatic epithelial cells through mitogen-activated protein kinase signaling pathways. Mol Cancer Res 7: 799-808, 2009.
29. Ren J, Li G, Ge J, Li X and Zhao Y: Is K-ras gene mutation a prognostic factor for colorectal cancer: A systematic review and meta-analysis. Dis Colon Rectum 55: 913-923, 2012.
30. Tsuchida N, Murugan AK and Grieco M: Kirsten Ras® oncogene: Significance of its discovery in human cancer research. Oncotarget 7: 46717-46733, 2016.
31. Deng Y, Wang L, Tan S, Kim GP, Dou R, Chen D, Cai Y, Fu X, Wang L, Zhu J, *et al*: KRAS as a predictor of poor prognosis and benefit from postoperative FOLFOX chemotherapy in patients with stage II and III colorectal cancer. Mol Oncol 9: 1341-1347, 2015.
32. Gil Ferreira C, Aran V, Zalcberg-Renault I, Victorino AP, Salem JH, Bonamino MH, Vieira FM and Zalis M: *KRAS* mutations: Variable incidences in a Brazilian cohort of 8,234 metastatic colorectal cancer patients. BMC Gastroenterol 14: 73, 2014.
33. Friedman RC, Farh KK, Burge CB and Bartel DP: Most mammalian mRNAs are conserved targets of microRNAs. Genome Res 19: 92-105, 2009.